

Spectral correlation in the adsorption of aliphatic mercaptans on silver and gold surfaces: Raman spectroscopic and computational study

Seung Il Cho, Eun Sun Park, Kwan Kim*, Myung Soo Kim

Department of Chemistry and Center for Molecular Catalysis, Seoul National University, Seoul 151-742, South Korea

Received 20 July 1998; accepted 12 November 1998

Abstract

Spectral shifts of the $\nu(\text{CS})$ vibrations of several aliphatic mercaptans adsorbed on the Ag and Au electrode surfaces were measured with the surface-enhanced Raman scattering. Influence of the chemisorption mechanism on the spectral shift was investigated through ab initio quantum mechanical calculation for CH_3SH , CH_3S^- , CH_3SNa , and CH_3SM_n ($M = \text{Ag, Au}$ and $n = 1-3$). It was found that even though the $2e$ molecular orbital of methanethiolate makes the major contribution to its chemisorption, the $3a_1$ orbital is mainly responsible for the $\nu(\text{CS})$ spectral shift. Adsorption of thiolates on the roughened Ag electrode surface seems to occur at the multiple sites such as the three-fold hollow sites while the number of the surface Au atoms interacting effectively with thiolates seems to be less than that of the Ag atoms. © 1999 Elsevier Science B.V. All rights reserved.

Keywords: Raman; Surface-enhanced Raman scattering; Aliphatic mercaptans; Ag; Au

1. Introduction

Adsorption of organic mercaptans on Ag and Au surfaces is the focus of tremendous research interest in relation to the preparation of well-organized organic thin films with practical applications [1–5]. Even though various spectroscopic tools are available to investigate such surface-adsorbate systems, there is none which is capable of providing all the answers relevant to the structure and bonding of the composite systems. This necessitates the use of several techniques in combination to elucidate the nature of the systems described before. For example, the structure on Ag or Au surface formed by self-assembling of

alkanethiolate was investigated by electron diffraction [6] and scanning tunneling microscopy [7,8]. Formation of a $\sqrt{3} \times \sqrt{3}R30^\circ$ structure was widely reported. Information on the orientation and order of polymethylene chains of the adsorbed alkanethiolates is available from infrared spectroscopy [9–11]. The tilt angles of $\sim 30^\circ$ and $\sim 12^\circ$ for monolayers on Au [9,11] and Ag [10,11], respectively, were reported, indicating a difference in the sulfur head group at the two metals. However, more direct information on the head group interaction is difficult to obtain from infrared spectroscopy. This is owing to the weak intensities of the C–S stretching ($\nu(\text{CS})$) and metal–sulfur stretching ($\nu(\text{MS})$) bands and other technical difficulties.

Surface-enhanced Raman scattering (SERS) which is known to be particularly sensitive to the vibrations

* Corresponding author. Tel.: + 82-2-880-6651; Fax: + 82-2-889-1568; e-mail: kwankim@plaza.snu.ac.kr

of atoms in the immediate vicinity of Ag and Au surfaces has also been applied to the investigation of the adsorption of organic mercaptans [12–16]. It was clearly shown by this technique that mercaptans chemisorb on the metal surfaces dissociatively after losing their thiol protons. Substantial red-shifts, namely the decrease in the vibrational frequencies, of the $\nu(\text{CS})$ modes were taken as an evidence for the participation of sulfur in the adsorption. Various theoretical efforts were made to understand the cause for such red-shifts and hence their adsorption mechanisms [17–19]. A consistent correlation between the spectral shift and the adsorption mechanism has not emerged yet, however. In this work, we present our recent results from the combined experimental and computational investigations on the adsorption of organic mercaptans on Ag and Au surfaces. A particular emphasis was placed on the consistent explanation of the spectral shift in terms of the adsorption mechanism.

2. Experimental

Samples investigated in this work are methanethiol, ethanethiol, propanethiol, buthanethiol, 2-methyl-2-propanethiol, and cyclohexanethiol, and their anions in the aqueous solutions. Ordinary Raman spectra of sodium, silver, and gold thiolate salts were also recorded. The sodium salts of methanethiolate, ethanethiolate, propanethiolate, buthanethiolate, and 2-methyl-2-propanethiolate were purchased from Fluka and washed thoroughly with ether. Sodium cyclohexanethiolate was prepared by mixing cyclohexanethiol with NaOH in methanol. Silver thiolate salts (R_SAg) were prepared by mixing an excess of sodium thiolate or thiol in methanol with AgNO₃ [20]. The resulting precipitates were washed thoroughly with methanol. Gold thiolate salts (R_SAu) were synthesized by the reduction of KAuCl₄ with thiol or thiolate in methanol [21]. The resulting precipitates were washed thoroughly with methanol and ether to remove disulfides. The metal-to-thiolate ratios were 1 : 1 in all the salts as determined by the Fajans method [22] and the elemental analysis.

The electrochemical system used to record SER spectra consists of three electrodes, a silver or gold working electrode, a platinum counter electrode, and a

saturated calomel reference electrode (SCE). A working electrode was prepared by polishing with sandpaper and with 0.05 μm alumina in distilled water and then oxidizing with equal volume mixture of 30% H₂O₂ and concentrated ammonia solution. The electrode was roughened in 0.1 M KCl solution by oxidation–reduction cycles. The electrochemical condition recommended by Gao et al. [23] was adopted. The electrode was immersed in 10⁻⁵ M thiolate solutions for 30 s. Then, the electrode was brought back into the electrochemical system. The potential of the working electrode was maintained at -0.2 V vs. SCE during SER spectral measurements even though the SER spectra were invariant with respect to the applied voltage. The reason for using separate solutions for adsorption and SER spectral recording is to avoid contamination of the electrochemical system with thiolates.

A sample was irradiated with a He/Ne laser (Research Electro-Optics Model LHRP-2001). The laser power was ~ 10 mW at the sample position. Raman scattering was collected at 90° using a $f/1.4$ camera lens with 50 mm focal length and focused onto the entrance slit of a Spex 1877E Triplemate spectrometer equipped with a charge-coupled device. The slit width was set at the spectral resolution of ~ 10 cm⁻¹. A commercial data system (Spex DM3000r), which was modified to improve cosmic ray rejection, was used for data acquisition and processing.

3. Computational

Ab initio molecular orbital calculation was done for CH₃SH, CH₃S⁻, CH₃SNa, CH₃SAg, CH₃SAg₂, CH₃SAg₃, CH₃SAu, CH₃SAu₂, and CH₃SAu₃ with the GAMESS package [24]. The 6-31G(3p, 3d) basis sets were used except for the gold and silver atoms. In order to reduce the amount of computation and to include some relativistic effects, the silver and gold atoms were treated with the effective core potentials of Stevens et al. [25] and the double or triple zeta basis sets recommended by them. The geometries of all the systems except for those containing two or three metal atoms were optimized at the Hartree–Fock (HF) level. For the latter, the metal–metal distance was fixed at 2.89 and 2.88 Å for silver and

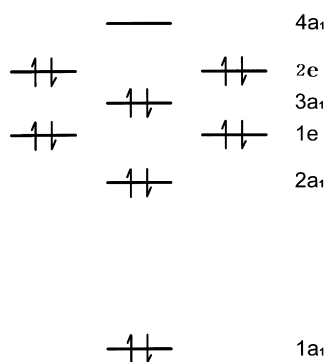


Fig. 1. A schematic energy diagram of the molecular orbitals of CH_3S^- .

gold, respectively, as taken from the bulk data [26], and other geometrical parameters were fully optimized. Harmonic vibrational frequencies were calculated at the optimized geometries.

4. Results and discussion

Before getting into the details of the present results, let us first review briefly the previous experimental and computational investigations [17–19] on the adsorption of aliphatic thiols, methanethiol in particular, on the Ag surface. For this purpose, a schematic energy diagram of the molecular orbitals of CH_3S^- is shown in Fig. 1. Herein, $1a_1$ is a bonding orbital formed between the s orbitals of carbon and sulfur. The $2a_1$ orbital is confined to the methyl group, possessing an antibonding character with respect to the C–S bond. The 1e's are degenerate bonding orbitals between the p_x and p_y orbitals of carbon and the 1s hydrogen atoms. The $3a_1$ orbital is a bonding orbital formed between the sp_z hybridized orbitals of carbon and sulfur atoms. The 2e orbitals, which are the highest occupied molecular orbitals (HOMO), are nonbonding orbitals virtually of p_x and p_y of sulfur with slight antibonding mixing from carbon p_x and p_y . Finally, $4a_1$, which is the lowest unoccupied molecular orbital (LUMO), is nearly a nonbonding orbital composed of p_z of carbon and s, p_z , and d_{z^2} of sulfur.

In our previous investigation on the adsorption of methanethiol on a silver surface, ab initio calculations were carried out for CH_3S^- , CH_3SAg , CH_3SAg_2 and other related molecules at the HF/6-31G* level [17].

The main interaction in the formation of the silver salts was identified as between the 2e orbitals of CH_3S^- and the LUMO of Ag^+ or Ag_2^+ . The calculated frequencies of the $\nu(\text{CS})$ mode followed the order $\text{CH}_3\text{SH} > \text{CH}_3\text{SAg} > \text{CH}_3\text{SAg}_2 > \text{CH}_3\text{S}^-$, in contrast with the experimental order $\text{CH}_3\text{SH} > \text{CH}_3\text{S}^- > \text{SERS}$. However, it was found through calculation that the $\nu(\text{CS})$ frequency of $\text{CH}_3\text{S}^- \text{--} \text{H}_2\text{O}$ was higher than that of free CH_3S^- . Hence, the experimental order $\text{CH}_3\text{S}^- > \text{SERS}$ was attributed to the hydration of CH_3S^- in aqueous solution. Another interesting theoretical investigation on the adsorption of CH_3S^- on silver was carried out by Lee et al. [18] using the atom superposition and electron delocalization molecular orbital (ASED-MO) calculation by modeling the Ag(111) and Ag(100) surfaces as clusters of 41–55 atoms. In particular, the reduced overlap population (ROP) of the chemisorption bond and the contribution from each MO of CH_3S^- were calculated. It was found that the chemisorption was mainly owing to the 2e and $3a_1$ MOs. Noting that the contribution from the 2e MO was larger by a factor of 3 than that from $3a_1$, it was suggested that electron donation from the 2e orbitals in the chemisorption would result in the blue-shift of the $\nu(\text{CS})$ mode of the adsorbed CH_3S^- compared to the free CH_3S^- . Then, our previous calculation on the $\text{CH}_3\text{S}^- \text{--} \text{H}_2\text{O}$ system [17] was invoked to explain the fact that the experimental order of the $\nu(\text{CS})$ frequencies was opposite to the calculated ones. An important point we would like to emphasize here is that the 2e orbitals are essentially nonbonding while $3a_1$ is bonding. Namely, even though the 2e orbitals make a large contribution to the chemisorption, it is possible that the C–S bond strength is more affected by the electron donation from $3a_1$. Also noteworthy in the work of Lee et al. [18] is that ROPs on the hollow sites are larger than those on the on-top sites both on the Ag(111) and Ag(100) surfaces indicating stronger chemisorption on the former.

The highest level calculation performed so far was reported by Sellers et al. [19] on the adsorption of CH_3S^- on Ag(100), Ag(111), Au(100), and Au(111) surfaces. Ab initio RECP HF + correlation with second-order perturbation theory (MBPT2) was adopted. The C–S axis of methanethiolate adsorbed on the hollow sites of all the surfaces was found to be perpendicular to the surfaces while it was tilted by

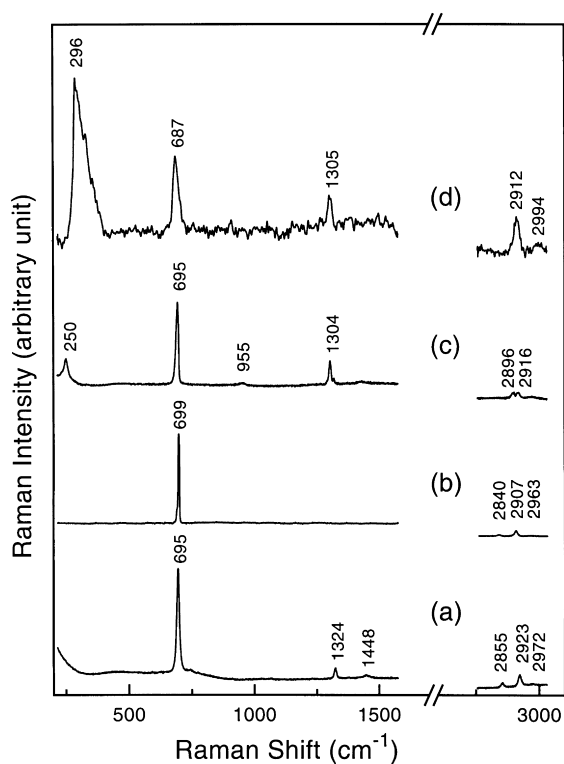


Fig. 2. Ordinary Raman spectra of (a) aqueous CH_3S^- and (b) sodium, (c) silver, and (d) gold salts of methanethiolate. The metal salts were rotated at 6000 rpm to minimize laser damage. The integration times were 2, 10, and 60 s for sodium, silver, and gold methanethiolate salts, respectively. The fluorescence background was subtracted.

$\sim 70^\circ$ from the surface normal when the adsorption occurred on the on-top sites. Adsorption on the hollow sites was a little bit more stable than on the on-top sites for all the surfaces investigated. For the same type of surfaces, the force constants for the $\nu(\text{CS})$ and $\nu(\text{MS})$ modes were larger on the Au surfaces than on Ag. However, the calculated results reported are not sufficient for the investigation of the spectral shifts upon surface adsorption.

The literature review shows that the quantum mechanical calculations present a consistent view on the chemisorption scheme regardless of the level of the calculations. This suggests that the misinterpretation of the calculated results, not the results themselves, may be responsible for the unsatisfactory explanation of the spectral shifts. Lack of experimental data such as the $\nu(\text{CS})$ frequency of free

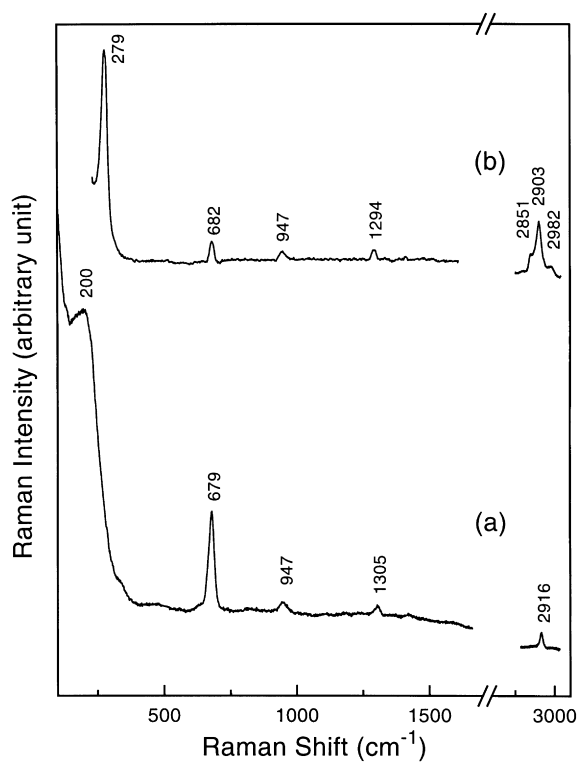


Fig. 3. SER spectra of methanethiolate on (a) Ag and (b) Au electrode surfaces. The integration times were 100 and 1000 s, respectively.

CH_3S^- may have caused such a misinterpretation. On these grounds, we prepared and measured the $\nu(\text{CS})$ frequencies of the sodium salts of aliphatic thioliates. The reason for studying these compounds was that the $\nu(\text{CS})$'s of these compounds would not be much affected by the presence of metal owing to the ionic nature of the Na–S bond and that these frequencies would provide better reference points to compare with than those for RS^- in aqueous solution which suffers from complication owing to hydration. Measurements were extended to several thiolate compounds to get a comprehensive view. Also, measurements were made for gold thiolate salts and for thioliates adsorbed on gold surfaces for comparison.

Ordinary Raman spectra of the sodium, silver, and gold salts of methanethiolate are shown in Fig. 2 together with the one for CH_3S^- in basic solution. The surface-enhanced Raman (SER) spectra of CH_3S^- adsorbed on Ag and Au electrode surfaces

Table 1
C–S stretching frequencies of aliphatic thiols

Compound	Ordinary Raman			SERS			
	RSH	RS ⁻	RSNa	RSAg	RSAu	Ag	Au
Methanethiol	705	695	699	695	687	679	682
Ethanethiol	658	656	663	645	646	630	643
Propanethiol (G) ^a	651	650	653	—	637	624	636
Propanethiol (T) ^a	733	728	732	716	720	697	707
Butanethiol (G) ^a	655	653	651	—	643	629	635
Butanethiol (T) ^a	731	734	724	718	718	697	702
Cyclohexanethiol (Eq.) ^b	735	732	733	729	724	712	721
2-Methyl-2-propanethiol	590	589	585	577	575	548	560

^a T and G denote the rotational isomers with *trans* and *gauche* conformations around the C(1)–C(2) bond, respectively.

^b Eq. denotes the equatorial conformation.

are shown in Fig. 3. The C–S stretching frequencies in these spectra and those in the corresponding spectra of other aliphatic thiolates are listed in Table 1. It is to be noted that the order of the C–S stretching frequency, RSH > RS⁻ > RSM > SERS (where M is Ag or Au) is observed for almost all the thiolates investigated. The $\nu(\text{CS})$ frequencies of the sodium salts are invariably higher than the corresponding frequencies of the silver or gold salts. These are higher than those of RS⁻ in the aqueous solution in some cases and lower in others. This may be owing to the difference in the extent of hydration of RS⁻ in aqueous solution as was suggested previously [17]. For example, the $\nu(\text{CS})$ frequency of CH₃S⁻ in the aqueous solution is lower than that of CH₃SNa. Also noteworthy is

the fact that the red-shifts for the Ag salts are comparable to or less than those for the corresponding Au salts. In contrast, the red-shifts on the Ag surfaces are invariably larger than those on the Au surfaces. The order of the $\nu(\text{CS})$ frequencies can be summarized as RSNa > RSAg \geq RSAu > RS-Au surface > RS-Ag surface. This result cannot be explained based on the previous chemisorption scheme of thiolates described before [17,18], necessitating further computation and interpretation of the computed results.

Structural data and $\nu(\text{CS})$ and $\nu(\text{MS})$ frequencies of various CH₃SM_{*n*} (M = Na, Ag, Au and *n* = 1, 2, 3) species obtained from ab initio molecular orbital calculations at the HF/6-31G(3p, 3d) level are listed in Table 2. The calculated harmonic frequencies

Table 2
Structure and frequencies of the CH₃S systems calculated at the HF level with 6-31G(3p, 3d) basis set^a

	AgSCH ₃	Ag ₂ SCH ₃	Ag ₃ SCH ₃	AuSCH ₃	Au ₂ SCH ₃	Au ₃ SCH ₃	NaSCH ₃
<i>r</i> SX ^b	2.4378	2.2228	2.8709	2.3273	2.1184	2.8828	2.5277
<i>r</i> CS	1.8283	1.8329	1.8316	1.8247	1.8324	1.8299	1.8298
<i>r</i> CH _{tr}	1.0836	1.0824	1.0828	1.0840	1.0822	1.0831	1.0837
<i>r</i> CH _g	1.0828	1.0818	1.0828	1.0812	1.0801	1.0831	1.0844
\angle CSX	106.16	113.08	144.47	104.94	111.96	144.77	111.24
\angle H _{tr} CS	107.51	108.25	110.00	106.24	107.56	109.95	108.79
\angle H _g CS	111.70	111.31	110.00	111.61	110.95	109.95	111.64
\angle H _{tr} CSX	180.00	180.00	180.00	180.00	180.00	180.00	180.00
\angle H _g CSX	61.37	60.81	60.00	61.70	60.91	60.00	61.00
C–S freq.	750	746	735	748	740.5	732.5	752
M–S freq.	298	225	160	342	241	157	310

^a Bond lengths (*r*) are in Å, angles (\angle) are in degrees, and frequencies are in cm⁻¹.

^b X = H for CH₃SH; X = Na, Ag, and Au for NaSCH₃, AgSCH₃, and AuSCH₃, respectively; X is the center of the two metal atoms for Ag₂SCH₃ and Au₂SCH₃; X is one of the three Ag or Au atoms for Ag₃SCH₃ or Au₃SCH₃.

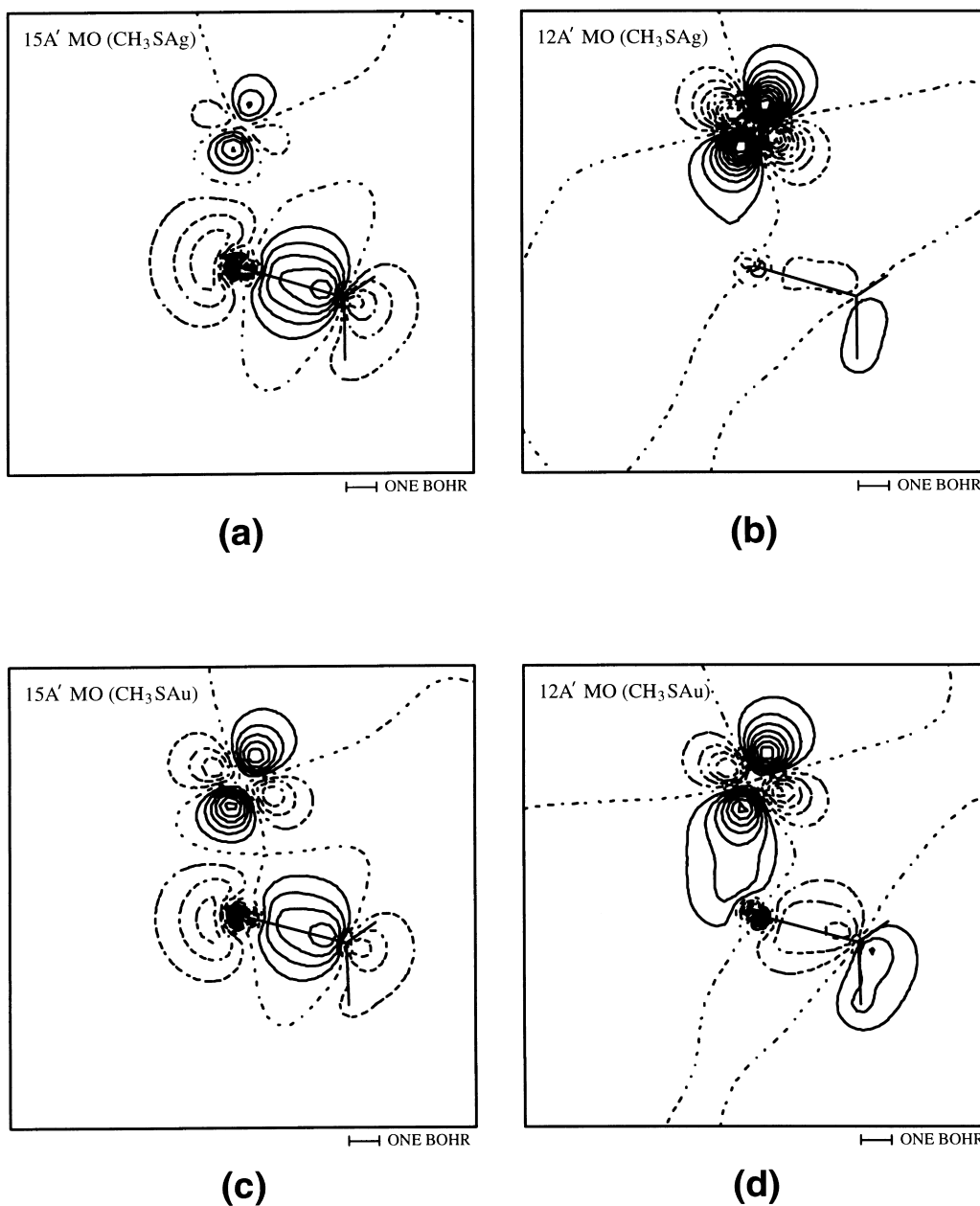


Fig. 4. Two-dimensional HF MO contour diagrams for CH₃SAg and CH₃SAu. In each plot, the contour spacing is 0.05 a.u. Solid lines denote contours of positive amplitude and dashed lines denote those of negative amplitude or nodal planes. The plotting plane contains four atoms, i.e., M (Ag or Au), S, C, and H_{trans}, which are connected by solid lines. The C–H_{gauche} bond is also shown by solid lines. (a) 15A' and (b) 12A' MOs for the CH₃SAg system. (c) 15A' and (d) 12A' MOs for CH₃SAu system.

would be $\sim 10\%$ higher than the real values, as is usual for the calculation at this level. It is to be borne in mind that the calculations are for CH_3SM_n molecular species while multiple interaction is possible between CH_3S^- and metal atoms in salt. Unfortunately, detailed structural information on Ag and Au salts of CH_3S^- from X-ray diffraction study is not available. In the case of silver hexanethiolate, an X-ray diffraction study shows that both the sulfur and silver are either two-fold or three-fold coordinated [27]. A closer inspection of the Ag–S distances shows, however, that the interaction of some pairs of Ag and S atoms is more important than others. No crystal structure information is available for gold thiolate salts. Considering the stoichiometry of salts, we would assume that sulfur atoms interact with one or two Ag or Au atoms in the salts. Namely, the C–S bonds in the salts may be closer to those in CH_3SM or CH_3SM_2 species considered in the calculation rather than those in CH_3SM_3 . It is informative at this point to compare the $\nu(\text{MS})$ modes which appear at 250 and 297 cm^{-1} , respectively, in the spectra of silver and gold salts of methanethiol (Fig. 2). The experimental frequency difference of 47 cm^{-1} , the $\nu(\text{AuS})$ being higher than the $\nu(\text{AgS})$, compares well with the corresponding difference between CH_3SAu and CH_3SAg in the calculation, suggesting that the CH_3SAu and CH_3SAg species may approximate the respective salts rather well.

It is interesting to note the order in the experimental $\nu(\text{CS})$ frequency of Na salt > Ag salt > Au salt. A similar trend, $\text{CH}_3\text{SNa} > \text{CH}_3\text{SAg} > \text{CH}_3\text{SAu}$, is seen in the calculated results also. According to the previous chemisorption model described earlier [17,18], the electron donation from the 2e orbitals of CH_3S^- to Ag or Au would result in the blue-shift of the $\nu(\text{CS})$ mode owing to the slight anti-bonding character of these orbitals with respect to the C–S bond. This is contrary to the experimental and computational findings. A feasible explanation for the red-shifts is to assume that the electron donation from the $3a_1$ orbital of CH_3S^- which is bonding with respect to the C–S bond is mainly responsible for the $\nu(\text{CS})$ frequency shift, even though the 2e orbitals contribute more to the chemisorption bond. As an attempt to obtain further support for this model, we compared the contours of $12A'$ and $15A'$ molecular orbitals of CH_3SAg and CH_3SAu species which are

formed by the interaction between $3a_1$ of CH_3S^- and d orbitals of the metals. The contour diagrams in Fig. 4 show that these orbitals are more delocalized in CH_3SAu than in CH_3SAg . Namely, its contribution to chemisorption is larger in CH_3SAu than in CH_3SAg , in agreement with the lower calculated $\nu(\text{CS})$ frequency in CH_3SAu than in CH_3SAg . It is worth mentioning that the $3a_1$ orbital in the sodium salt is virtually the same as in the free anion, hardly affected by the presence of Na^+ .

As was mentioned earlier, the red-shifts of the $\nu(\text{CS})$ mode on the electrode surfaces are larger than in the salts. In addition, the red-shift on the silver surface is larger than that on the gold surface. According to Sellers et al. [19], the bonding of the sulfur atom at the on-top site of various surfaces is concentrated upon a single metal atom. Then, the metal salts considered before would approximate the bonding at these sites rather well. The fact that the red-shifts are larger on the surfaces than those in salts suggests that the adsorption on the surfaces occurs at the multiple sites such as two-fold or three-fold sites. In this respect, some knowledge is needed on the structures of the metal surfaces used. Considering the microscopic roughness needed for a successful SERS investigation, the presence of a mixture of surface planes would not be surprising, however. According to the investigations with the scanning tunnelling microscopy, the surface structures of Ag and Au metals are predominantly consisting of the (111) planes [7,28]. Similar results were reported for the evaporated films of Ag [29] and Au [29,30]. No experimental result on the structure of the electrode surfaces roughened by oxidation–reduction cycles is available. It seems reasonable, however, to assume the predominance of the (111) planes as in films. Then, it would be desirable to carry out an ab initio calculation for CH_3S –metal cluster systems which can closely mimic the adsorption of methanethiolate on (111) metal surface planes. At the current level of calculation, we faced difficulty related to the convergence in the SCF iteration when more than three metal atoms were included. Hence, to gain an insight into the adsorption of CH_3S^- at the three-fold sites on the (111) planes, calculated results for CH_3SM_3 was compared with those for CH_3SM and CH_3SM_2 . The results in Table 2 show that the $\nu(\text{CS})$ frequency red-shifts more as the number of the metal atoms, either

Ag or Au, coordinated to methanethiolate increases. This is in agreement with the experimental observation that this mode for methanethiolate adsorbed on the metal surfaces appears at lower frequencies compared to those for the respective salts. In particular, the red-shifts of this mode for CH_3SAg_3 from the one for CH_3SAg is comparable to the experimental frequency difference between the silver salt and SERS. As was mentioned earlier, the substantial red-shifts of this mode in SERS compared to those in salts are observed in all the thiolates investigated in this work. This led us to conclude that the adsorption of the thiolates on the roughened silver electrode surfaces occurs mainly on the multiple sites, the three-fold hollow sites in particular.

In the case of Au, however, the experimental $\nu(\text{CS})$ frequency difference between the salts and SERS is generally smaller than that between CH_3SAu and CH_3SAu_3 in the calculated results. The $\nu(\text{CS})$ frequencies on the Au electrode surfaces are invariably higher than the corresponding ones on Ag for all the thiolates investigated. In contrast, the calculated $\nu(\text{CS})$ frequencies for CH_3SAu_n are lower than the corresponding values for CH_3SAg_n for $n = 1, 2,$ and 3 . These results can be reconciled only by assuming that the three-fold sites on the Au electrode surfaces are not as much favored as those on Ag for the adsorption of thiolate. This may imply that adsorption of CH_3S^- on the Au electrode surface occurs mostly on the on-top or two-fold bridge sites.

In the electron energy loss spectroscopic study on the adsorption of dimethyl disulfide on Au(111) [31], the molecule was found to adsorb dissociatively with the C–S bond of the thiolate tilted from the surface normal. Contrarily, the perpendicular orientation of the C–S bond of methanethiolate with respect to the Ag(111) surface was observed by the sum frequency generation spectroscopy [32]. Similar trend was suggested for the adsorption of alkanethiolates with long chains by the quantitative analysis of the infrared spectral data [9–11]. According to the high level *ab initio* study by Sellers et al. [19], the C–S surface angles for methanethiolate adsorbed at the on-top sites of Ag(111) and Au(111) planes are $\sim 105^\circ$, while those at the hollow sites are 180° . Combining these experimental and computational results, one finds that the adsorption of methanethiolate occurs mostly at the on-top sites on Au while at the hollow

sites on Ag. This is in agreement with our results from the analysis of the spectral shift described earlier. Also noteworthy is the fact that the relative intensity of the $\nu(\text{CS})$ mode on the gold electrode is weaker than that on the silver electrode (see Fig. 3). According to the electromagnetic selection rule for SERS proposed by Creighton [33] and by Moskovits and Suh [34], vibrations with nonvanishing tensor components along the surface normal display larger enhancement in their Raman intensities than others. This is in agreement with the present results. However, it is well known that the surface enhancement is also affected by other factors such as the charge transfer [35].

According to the calculation by Sellers et al. [19], adsorption at the hollow sites is energetically more favorable than that at the on-top sites, slightly more so on Au(111) than on Ag(111). Hence, it is difficult to understand why multiple sites on the Au electrode surfaces are less favored than those on the Ag electrode. One can guess that it may have something to do with the fact that the valence orbitals of atomic silver are significantly more diffuse and extend higher above the surface than those of gold. Nonetheless, it should be recalled that even though the $\nu(\text{CS})$ frequencies of all the thiolates on the Au surfaces are consistently higher than the corresponding values on the Ag surfaces, the frequency difference between the gold salts and those on the Au surfaces are very diverse. For example, rather small differences are observed for methanethiol, ethanethiol, propanethiol (G), butanethiol (G), and cyclohexanethiol, while substantially larger differences are seen for propanethiol (T), butanethiol (T), and 2-methyl-2-propanethiol. Hence, we cannot generalize on the nature of the binding sites on the Au surfaces. All that can be said is that the number of atoms on the Au surface contributing to the chemisorption of thiolates is smaller on the average than those on the Ag surface.

It was well documented that the crystal structure of the surface of the gold substrate does influence the structure of the self-assembled alkanethiol monolayers. For instance, from a helium atom diffraction study the alkyl chains were concluded to be more tilted from the surface normal on a Au(110) surface than on Au(111) [36]. Contrarily, the alkyl chains were packed more densely on Au(100) than on Au(111) and (110) surfaces [6,36,37]. In this respect,

the detailed structure of the roughened gold electrode has to be clarified in the near future to understand the shift of the C–S stretching frequencies of alkanethiolates on gold more precisely.

5. Conclusion

Methanethiolate chemisorbs on the Ag or Au surfaces mainly via its 2e and 3a₁ molecular orbitals. The 2e orbitals are virtually nonbonding with respect to the C–S bond possessing only a slight antibonding character, while the 3a₁ orbital is bonding. Hence, even though the 2e orbitals contribute more to the chemisorption than the 3a₁ orbital, the frequency shift of the $\nu(\text{CS})$ mode is more affected by the electron donation from the latter than from the former. In the case of the Ag surface, adsorption of thiolates seems to occur at the multiple sites, such as the three-fold hollow sites. The nature of the adsorption sites on the Au surfaces is less clear, being more or less adsorbate dependent, even though the number of the Au atoms interacting with thiolates are less than that of the Ag atoms on the average.

Acknowledgements

This work was supported by the Korea Science and Engineering Foundation through the Center for Molecular Catalysis at Seoul National University (SNU) and by the Korea Research Foundation through the Basic Science Research Institute at SNU.

References

- [1] G.M. Whitesides, P.E. Laibinis, *Langmuir* 6 (1990) 87.
- [2] A. Ulman, *An Introduction to Ultrathin Organic Films from Langmuir–Blodgett to Self-Assembly*, Academic Press, Boston, 1991.
- [3] L.H. Dubois, R.G. Nuzzo, *Annu. Rev. Phys. Chem.* 43 (1992) 437.
- [4] C.A. Alves, E.L. Smith, M.D. Porter, *J. Am. Chem. Soc.* 114 (1992) 1222.
- [5] A. Ulman, *Chem. Rev.* 96 (1996) 1533.
- [6] L.H. Dubois, B.R. Zegarski, R.G. Nuzzo, *J. Chem. Phys.* 98 (1993) 678.

- [7] C.A. Widrig, C.A. Alves, M.D. Porter, *J. Am. Chem. Soc.* 113 (1991) 2805.
- [8] R. Heinz, J.P. Rabe, *Langmuir* 11 (1995) 506.
- [9] M.D. Porter, T.B. Bright, D.L. Allara, C.E.D. Chidsey, *J. Am. Chem. Soc.* 109 (1987) 3359.
- [10] M.M. Walczak, C. Chung, S.M. Stole, C.A. Widrig, M.D. Porter, *J. Am. Chem. Soc.* 113 (1991) 2470.
- [11] P.E. Laibinis, G.M. Tjatjopoulos, D.L. Allara, Y. Tao, A.N. Parikh, R.G. Nuzzo, *J. Am. Chem. Soc.* 113 (1991) 7152.
- [12] T.H. Joo, K. Kim, M.S. Kim, *J. Phys. Chem.* 90 (1986) 5816.
- [13] C.K. Kwon, K. Kim, M.S. Kim, *J. Mol. Struct.* 197 (1989) 171.
- [14] S.H. Cho, H.S. Han, D.-J. Jang, K. Kim, M.S. Kim, *J. Phys. Chem.* 99 (1995) 10594.
- [15] M.A. Bryant, J.E. Perberon, *J. Am. Chem. Soc.* 113 (1991) 8284.
- [16] C.A. Szafranski, W. Tanner, P.E. Laibinis, R.L. Garrell, *Langmuir* 14 (1998) 3570.
- [17] S.B. Lee, K. Kim, M.S. Kim, W.S. Oh, Y.S. Lee, *J. Mol. Struct.* 296 (1993) 5.
- [18] K. Lee, S. Park, H. Kim, *Bull. Kor. Chem. Soc.* 16 (1995) 89.
- [19] H. Sellers, A. Ulman, Y. Shnidman, J.E. Eilers, *J. Am. Chem. Soc.* 115 (1993) 9389.
- [20] T.H. Joo, M.S. Kim, K. Kim, *J. Raman Spectrosc.* 18 (1987) 57.
- [21] R. Puddephatt, *The Chemistry of Gold*, Elsevier, Oxford, 1978.
- [22] D.C. Harris, *Quantitative Chemical Analysis*, Freeman, New York, 1995.
- [23] P. Gao, D. Gosztola, L.H. Leung, M.J. Weaver, *J. Electroanal. Chem.* 243 (1987) 211.
- [24] M.W. Schmitt, K.K. Baldrige, J.A. Boatz, S.T. Elbert, M.S. Gordon, J.H. Jensen, S. Koseki, N. Matsunaga, K.A. Nguyen, S.J. Su, T.L. Windus, M. Dupuis, J.A. Montgomery, *J. Comput. Chem.* 14 (1993) 1347. Original program assembled by the staff of the NRCC: M. Dupuis, D. Spangler, J.J. Wendoloski, National Resource for Computations in Chemistry Software Catalog Program QG01, University of California, Berkeley, CA, 1980.
- [25] W.J. Stevens, H. Basch, M. Krauss, P. Jasien, *Can. J. Chem.* 70 (1992) 612.
- [26] A.G. Massey, N.R. Thompson, B.F.G. Johnson, R. Davis, *The Chemistry of Copper, Silver, and Gold*, Pergamon, Oxford, 1973.
- [27] S.H. Hong, U.Z. Olin, R. Hesse, *Acta Chem. Scand. A* 29 (1975) 583.
- [28] V.N. Hallmark, S. Chiang, J.F. Rabolt, J.D. Swalen, R. Wilson, *J. Phys. Rev. Lett.* 59 (1987) 2879.
- [29] S. Buchholz, H. Fuchs, J.P. Rabe, *J. Vac. Sci. Technol. B* 9 (1991) 857.
- [30] M.S. Zei, Y. Nakai, G. Lehmpfuhl, D.M. Kolb, *J. Electroanal. Chem.* 150 (1983) 201.
- [31] R.G. Nuzzo, B.R. Zegarski, L.H. Dubois, *J. Am. Chem. Soc.* 109 (1987) 733.

- [32] A.L. Harris, L.H. Rothberg, L.H. Dubois, N.J. Levinos, L. Dhar, *Phys. Rev. Lett.* 64 (1990) 2086.
- [33] J.A. Creighton, *Surf. Sci.* 124 (1983) 209.
- [34] M. Moskovits, J.S. Suh, *J. Phys. Chem.* 88 (1984) 5526.
- [35] R.L. Birke, T. Lu, J.R. Lombardi, in: R. Varma, J.R. Selman (Eds.), *Techniques for Characterization of Electrodes and Electrochemical Processes*, Wiley, New York, 1991, p. 211.
- [36] N. Camillone, C.E.D. Chidsey, G.-Y. Liu, G. Scoles, *J. Chem. Phys.* 98 (1993) 4234.
- [37] L. Strong, G.M. Whitesides, *Langmuir* 4 (1988) 546.